ELSEVIER

Journal of Organometallic Chemistry 566 (1998) 103–110

Journal of Organo metallic Chemistry

Synthesis, structures and in vitro antitumor activity of some germanium-substituted di-*n*-butyltin dipropionates

Song Xueqing *, Yang Zhiqiang, Xie Qinglan, Li Jinshan

National Laboratory of Elemento-Organic Chemistry, NanKai University, Tianjin, 300071, People's Republic of China

Received 20 February 1998

Abstract

Sixteen new germanium-substituted di-*n*-butyltin dipropionates with the form $(R_3GeCHR^2CHR^1COO)_2SnBu^n_2.H_2O$ ($R_3 = Ph_3$, $N(OCH_2CH_2)_3$; $R^2 = H,CH_3$, Aryl; $R^1 = H,CH_3$) were synthesized and characterized by IR, NMR (^1H, ^{119}Sn) and MS spectroscopy, and in the case of $^nBu_2Sn[O_2CCH_2CH(4\text{-}Cl\text{-}C_6H_4)Ge(OCH_2CH_2)_3N]_2.H_2O$ by X-ray diffraction study. The in vitro antitumor activity of some selected derivatives against KB cells, HCT-8 cells and Bel7402 cells is presented. © 1998 Elsevier Science S.A. All rights reserved.

Keywords: di-*n*-Butyltin dipropionates; Infrared spectroscopy; Crystal structure; Antitumor activity

---

1. Introduction

The study of organotin compounds is of current interest owing to their wide range of applications [1–4] such as biocides and as homogeneous catalysts in industry. Recently, the potential antitumor activity of diorganotin carboxylates has been widely studied [5]. As we know very well, organogermanium is another kind of element that has a wide range of biological activity [6]. Therefore, we here prepared 16 new germanium-substituted di-*n*-butyltin dipropionates in order to examine whether including germanium into the diorganotin compounds improves their antitumor properties. In parallel, we were also interested in studying the nature of bonding and structure of these compounds.

These germanium-substituted di-*n*-butyltin dipropionates were synthesized by the condensation of di-*n*-butyltin oxide and germanium-substituted propionic acids in the molar ratio 1:2. The general reaction scheme is shown as following:

$$^nBu_2SnO + 2HO_2CCHR^1CHR^2GeR_3$$
$$\rightarrow {}^nBu_2Sn(O_2CCHR^1CHR^2GeR_3)_2.H_2O$$

For compounds I, $R_3 = (OCH_2CH_2)_3N$, $R^1 = H$, and R^2 is: H (I_1); CH_3 (I_2); C_6H_5 (I_3); 4-ClC_6H_4 (I_4); 2-ClC_6H_4 (I_5); 4-$CH_3C_6H_4$ (I_6); 2-$CH_3C_6H_4$ (I_7); 2,4-$Cl_2C_6H_3$ (I_8); 4-$CH_3OC_6H_4$ (I_9); 4-$NO_2C_6H_4$ (I_{10}); $R^1 = CH_3$, $R^2 = H$ (I_{11}). For compounds II, $R_3 = Ph_3$, $R^1 = H$, and R^2 is: CH_3 (II_1); C_6H_5 (II_2); 4-ClC_6H_4 (II_3); 4-$CH_3C_6H_4$ (II_4); 4-$CH_3OC_6H_4$ (II_5).

2. Experimental section

2.1. Instruments

IR spectra were recorded on a Shimadzu IR-435 spectrometer in KBr discs. The ^1H-NMR and ^{119}Sn-NMR spectra were measured on a JEOL-FX-90Q spectrometer with TMS as internal and Me_4Sn as external standard. Elemental analyses were determined on an MT-3 elemental analyzer. Mass spectra were recorded on an HP-5988A at 70 ev, the temperature of ionization was 200°C.

---

* Corresponding author.

PII S0022-328X(98)00607-X

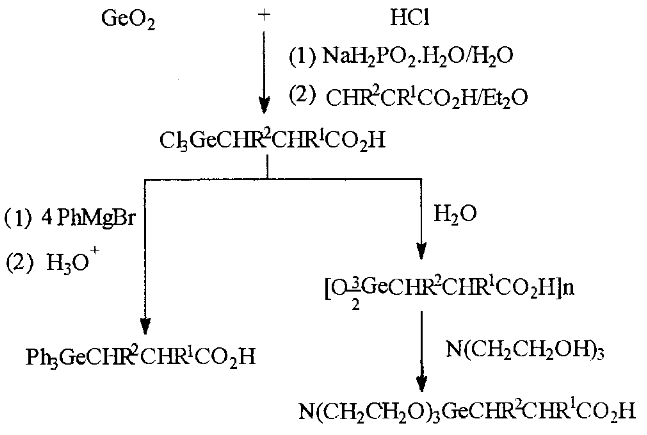

Scheme 1.

2.2. Synthesis

Di-*n*-butyltin oxide was prepared by alkaline hydrolysis of $^n\mathrm{Bu_2SnCl_2}$, and the germanium-substituted propionic acids were prepared according to earlier reference [7] (see Scheme 1).

The synthesis of compounds I and II is analogous to that of diorganotin dicarboxylates. Typically, 0.005 mol di-*n*-butyltin oxide was suspended in a solution of 0.01 mol of the appropriate substituted propionic acid in 200 ml of toluene and refluxed for 6 h, one half of the solvent was distiled off with a Dean–Stark apparatus. The remaining homogeneous solution was then cooled off and filtered. The solvent was evaporated under vacuum. The obtained solid was recrystallized from solvent mixture $CHCl_3$/petroether. The yields, physical states, melting points and elemental analyses of the prepared compounds are given in Table 1.

Table 2
IR data of carbonyl groups of $^n\mathrm{Bu_2Sn(O_2CCHR^1CHR^2GeR_3)_2.H_2O}$ (cm^{-1})

Compound	υ asym	υ sym	$\Delta\ \upsilon$	υ_{H-O-H}
I_1	1623	1379	244	3357
	1552	1407	145	
I_6	1631	1366	259	3382
	1562	1398	156	
I_7	1631	1361	270	3396
	1559	1404	155	
I_9	1638	1366	272	3401
	1562	1398	164	
I_{10}	1627	1339	288	3386
	1566	1401	165	
II_3	1635	1337	298	3400
	1558	1380	188	
II_5	1605	1331	274	3394
	1563	1397	166	
I_{11}	1604	1389	215	3377
I_2	1595	1395	200	3362
I_3	1578	1382	196	3394
I_4	1592	1378	214	3385
I_5	1591	1384	207	3382
I_8	1595	1382	213	3403
II_1	1578	1366	212	3388
II_2	1590	1379	211	3406
II_4	1614	1376	238	3400

2.3. Crystal structure determination

Intensity data for colorless crystal (0.25 × 0.3 × 0.3 mm) of $^n\mathrm{Bu_2Sn[O_2CCH_2CH(4\text{-}ClC_6H_4)Ge(OCH_2CH_2)_3N]_2.H_2O}$ were measured at 299 K on an Enraf-Nonius CAD4F diffractometer fitted with graphite-monochromatized Mo–K_α radiation. $\lambda = 0.71073$. The $\omega{:}2\theta$ scan technique was employed to measure 3319 data up to a maximum Bragg angle of 23°. The data set was corrected for Lorentz and polarization effects and for

Table 1
The yields and elemental analyses of $^n\mathrm{Bu_2Sn(O_2CCHR^1CHR^2GeR_3)_2.H_2O}$

Number	Physical state	MW	Yield (%)	Mp. (°C)	(C%) Analysis	(H%) Elemental	(N%) Found (Calcd.)
I_1	White crystal	832.57	91.7	152–154	37.88(37.51)	6.22(6.30)	3.16(3.36)
I_2	White crystal	860.87	89.3	164–166	39.45(39.07)	6.42(6.56)	3.35(3.26)
I_3	White crystal	984.77	93.5	236–239	46.78(46.35)	5.54(6.14)	2.78(2.84)
I_4	White crystal	1053.66	71.2	241–243	43.40(43.16)	5.55(5.52)	2.68(2.65)
I_5	White crystal	1053.66	88.4	218–220	43.63(43.16)	5.40(5.52)	2.80(2.65)
I_6	White crystal	1122.55	76.4	240–242	40.57(40.66)	5.04(5.03)	2.08(2.50)
I_7	White crystal	1012.82	84.5	245–246	47.59(47.43)	6.49(6.17)	2.32(2.77)
I_8	White crystal	1012.82	91.5	217–219	47.81(47.43)	6.54(6.17)	2.75(2.77)
I_9	White crystal	1044.82	90.3	223–225	46.90(46.80)	6.30(6.09)	2.86(2.73)
I_{10}	White crystal	1106.42	87.3	244–246	41.48(41.24)	5.12(5.28)	4.60(5.06)
I_{11}	White crystal	860.87	80.6	187–189	39.51(39.07)	6.09(6.56)	3.20(3.26)
II_1	White crystal	1030.93	87.6	119–121	60.69(60.58)	6.15(6.06)	
II_2	White crystal	1155.07	80.9	150–153	64.75(64.47)	5.60(5.76)	
II_3	White crystal	1223.96	82.5	153–155	65.26(64.97)	6.01(5.90)	
II_4	White crystal	1183.13	85.4	96–98	63.29(63.27)	5.82(5.64)	
II_5	White crystal	1114.86	76.1	161–163	61.35(60.86)	5.34(5.27)	

For compounds of type I, $R_3 = (OCH_2CH_2)_3N$; for compounds of type II, $R_3 = Ph_3$.

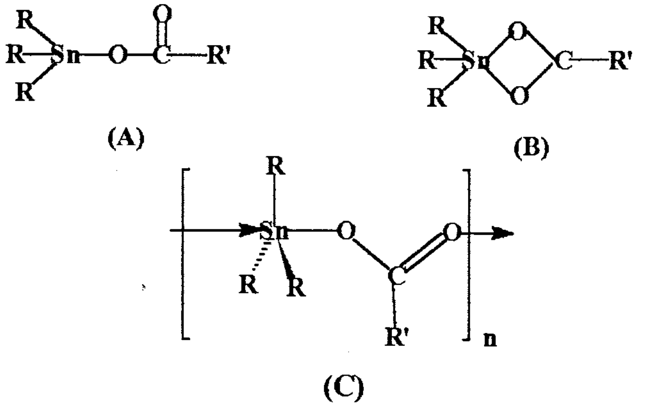

Scheme 2.

absorption using an analytical procedure, maximum and minimum transmission factors were 0.641 and 0.591, respectively. There were 2760 independent reflections of which 1819 satisfied the $I \geq 3\sigma(I)$ criterion and were used in the subsequent analysis.

Crystal data for $^{n}Bu_2Sn[O_2CCH_2CH(4\text{-}ClC_6H_4)Ge(OCH_2CH_2)_3N]_2.H_2O$: monoclinic, space group $C/2c$, $a = 21.182(5)$ Å, $b = 12.174(3)$ Å, $c = 17.108(4)$ Å, $\beta = 99.59(2)°$, $V = 4350(3)$ Å^3, $Z = 4$, $D_{calc.} = 1.581 mg\ m^{-3}$, $F(000) = 2104$, $\mu = 2.104\ mm^{-1}$.

The structure was solved from the interpretation of the patterns on synthesis and refined by a full-matrix least squares procedure based on F. Non-hydrogen atoms were refined with anisotropic thermal parameters. Hydrogen atoms were not included in the model. The refinement was continued with sigma weights until $R = 0.045$ and $Rw = 0.055$. The maximum residual electron density peak in the final difference map was 0.54 eÅ^{-3}. Final fractional atomic coordinates for the hydrogen atoms are listed in Table 8.

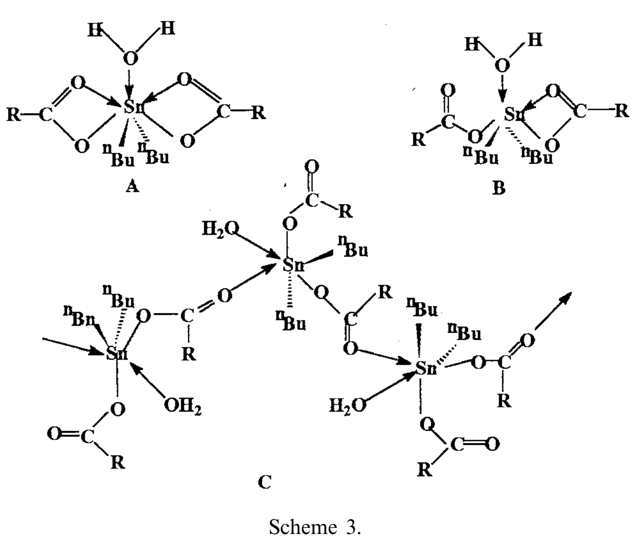

Scheme 3.

3. Results and discussion

3.1. IR data

The infrared spectra of these compounds have been recorded in the range of 4000–400 cm^{-1}. Tentative assignments have been made on the basis of earlier publications and important data are listed in Table 2. The absorptions of interest are those of carbonyl C=O, Sn–C, Sn–O and H–O–H bonds. In the spectra, medium to weak bands in the region 430–480 cm^{-1} are assigned to Sn–O [8]; those in the region 500–600 cm^{-1} indicate the presence of Sn–C bonds [9]. As there are wide and strong absorptions around 3400 cm^{-1}, we assume that there may be a water molecule in the product [10].

We know very well that there are mainly three kinds of structures for trialkyltin carboxylates [11]: the four-coordinate structure for the monomers (A) and the five-coordinate structure (B) for monomers and (C) for polymers (see Scheme 2).

The vacant 5d orbitals on tin atoms tend towards high-coordination with ligands containing lone electron pairs. The IR stretching vibration frequencies of carbonyl groups in organotin carboxylates are important for determining their structures: when the structure changes from A to B or C, the asymmetric absorption vibration frequencies (υ asym) of carbonyl groups decrease and the symmetric absorption vibration frequencies (υ sym) increase. The difference ($\Delta\ \upsilon_{C=O}$) therefore decreases.

The carbonyl absorptions of diorganotin carboxylates are apparently more complicated than those of trialkyl carboxylates, because there are two carbonyl groups. Therefore, if the two carbonyl groups have the same coordination environment, there is only one carbonyl absorption in the IR spectra; if there are two carbonyl absorptions in the spectra, the two carbonyl groups have different coordination environments [12].

We see from Table 2 that there are two types of carbonyl absorption in the list, one type has two carbonyl absorptions, and the other has only one. This suggests three types of structure for these compounds. Those of the di-*n*-butyltin dipropionates which have only one carbonyl absorption is illustrated as A, including the possibility of having a water molecule in the structure. Those having two carbonyl absorptions may be illustrated as B (intramolecular coordination) and C (intermolecular coordination) (see Scheme 3).

3.2. ^{1}H-NMR

The ^{1}H-NMR data of compounds II are presented in Table 3, and those of compounds I in Table 4. The butyltin derivatives show a multiplet in the region 0.68–1.48 ppm for butyl protons with a well defined

Table 3
Main ^{1}H-NMR data of ^{n}Bu$_2$Sn(O$_2$CCHR^{1}CHR^{2}GePh$_3$)$_2$.H$_2$O[a] (ppm)

Number	δ^1H					
	CH$_3$	(CH$_2$)$_3$	CH$_2$	CH	R^2	Ph
II$_1$	0.83(6H,t)	1.10–1.40(12H,m)	2.40–2.60(4H,m)	2.20–2.40(2H,m)	1.60(6H,d)	7.28(30,s)
II$_2$	0.72(6H,t)	1.04–1.28(12H,m)	2.96(4H,d)	3.72(2H,t)	6.80–7.20(10H,m)	7.35(30,s)
II$_3$	0.73(6H,t)	1.04–1.28(12H,m)	2.94(4H,d)	3.58(2H,t)	6.62–7.00(8H,dd)	7.22(30,s)
II$_4$	0.68(6H,t)	0.96–1.28(12H,m)	2.95(4H,d)	3.64(2H,t)	6.68–7.02(8H,dd) 2.27(6H,s)	7.36(30,s)
II$_5$	0.68(6H,t)	0.98–1.28(12H,m)	2.96(4H,d)	3.62(2H,t)	6.60–6.94(8H,dd) 3.76(6H,s)	7.38(30,s)

[a] R^1 = H.

Table 4
Main ^{1}H-NMR data for ^{n}Bu$_2$Sn[O$_2$CCHR^{1}CHR^{2}Ge(OCH$_2$CH$_2$)$_3$N]$_2$.H$_2$O (ppm)

Number	δ^1H						
	CH$_3$	(CH$_2$)$_3$	R^2(R^1)	CH and CH$_2$		N(CH$_2$)$_3$	(OCH$_2$)$_3$
I$_1$	0.87(6H,t)	1.12–1.48(12H,m)		2.60(4H,t)	1.64(4H,t)	2.84(12H,t)	3.78(12H,t)
I$_2$	0.90(6H,t)	1.14–1.48(12H,m)	1.26(6H,d)	1.64–1.78(2H,m)	2.65–2.86(4H,m)	2.80(12H,t)	3.78(12H,t)
I$_3$	0.78(6H,t)	1.04–1.46(12H,m)	7.04–7.44(10H,m)	3.04(6H,s)		2.78(12H,t)	3.76(12H,t)
I$_4$	0.78(6H,t)	1.06–1.34(12H,m)	7.04–7.40(8H,m)	3.00(6H,s)		2.76(12H,t)	3.72(12H,t)
I$_5$	0.78(6H,t)	1.02–1.36(12H,m)	6.94–7.60(8H,m)	3.04(6H,s)		2.78(12H,t)	3.74(12H,t)
I$_6$	0.76(6H,t)	0.98–1.20(12H,m)	7.00–7.48(6H,m)	3.06(6H,s)		2.77(12H,t)	3.79(12H,t)
I$_7$	0.78(6H,t)	0.96–1.18(12H,m)	7.00–7.16(8H,dd),2.24(6H,s)	3.00(6H,s)		2.78(12H,t)	3.76(12H,t)
I$_8$	0.76(6H,t)	0.96–1.18(12H,m)	7.00–7.46(8H,m),2.36(6H,s)	3.08(6H,s)		2.78(12H,t)	3.78(12H,t)
I$_9$	0.78(6H,t)	1.02–1.22(12H,m)	6.76–7.38(8H,dd),3.78(6H,s)	3.00(6H,s)		2.78(12H,t)	3.77(12H,t)
I$_{10}$		0.64–1.60(18H,m)	7.35–7.98(8H,m)	3.04(6H,s)		2.76(12H,t)	3.64(12H,t)
I$_{11}$	0.92(6H,t)	1.12–1.44(12H,m)	1.28(6H,d)[a]	2.72–2.86(2H,m)	1.70(4H,t)	2.82(12H,t)	3.80(12H,t)

For compound I$_1$ to I$_{10}$, R^1 = H; for compound I$_{11}$, R^2 = H.
[a] R^1 = CH$_3$.

Table 5
^{119}Sn-NMR data for ^{n}Bu$_2$Sn(O$_2$CCHR^{1}CHR^{2}GeR$_3$)$_2$.H$_2$O(ppm) (CDCl$_3$ as solvent)

	I$_3$	I$_4$	I$_7$	I$_9$	I$_{11}$	II$_1$	II$_2$	II$_3$	II$_4$	II$_5$
δ^{119}Sn	−150.7	−149.2	−200.9[a]	−151.4	−161.8	−146.4	−145.8	−144.6	−146.7	−146.8

[a] CDCl$_3$ + DMSO-d_6 as solvent.

triplet in the region 0.68–0.92 ppm, which may be due to the terminal methyl protons [13]. From the table we find that when one β proton is substituted with an aryl group, there is a significant downfield shift for the α and β protons due to the deshielding effects. Compare ^{1}H-NMR spectra of N(CH$_2$CH$_2$O)$_3$GeCHR^{2}CHR^{1}CO-OH with that of its derivatives [N(CH$_2$CH$_2$O)$_3$GeCHR^2 CHR^{1}CO$_2$]$_2$SnBu$^n_2$.H$_2$O, we find an upfield shift for the protons in N(CH$_2$CH$_2$O)$_3$Ge moiety. Here C(1) is a chiral center and C(2) is a prochiral center, and the three hydrogens on C(1) and C(2) comprise an ABC system. However, the ABC system can not be identified in 90 MHz spectra. Here the three hydrogens show a singlet in most cases. All the protons in the compounds have been identified and the total number of protons calculated from the integration curve tallies with what was expected from the molecular formula.

3.3. ^{119}Sn-NMR data

All the compounds selected for the ^{119}Sn-NMR study exhibit a single resonance in the region −140 to −165 ppm, except the compound I$_7$, which is only poorly soluble in CDCl$_3$, and exhibits a single resonance in DMSO-d_6 at a much higher field (as shown in Table 5), which may be attributed to the coordination of the DMSO-d_6 to tin atom [14]. Compared with previously published results [15], the shift range of these compounds looks more like pentacoordination. This suggests that all appear to have the same structure

Table 6
Main fragment ions observed for compounds I_3 and II_2

Compound I_3			Compound II_2		
m/z	Fragment ion	Intensity	m/z	Fragment ion	Intensity
602	$N(C_2H_4O)_3GeCHPhCH_2CO_2\overset{+}{Sn}Bu_2$	11	689	$Ph_3GeCH(C_6H_5)CH_2CO_2\overset{+}{Sn}Bu^n_2$	3.9
387	$PhCH{=}CHCOO\overset{+}{Sn}Bu^n_2$	51.7	305	Ph_3Ge^+	100
352	$N(C_2H_4O)GeCHPhCH_2C{\equiv}O^+$	10.5	267	$PhCH{=}CHCOO\overset{+}{Sn}$	5.7
267	$PhCH{=}CHCOO\overset{+}{Sn}$	16	234	$^nBu_2Sn^{+\cdot}$	7.4
220	$N(CH_2CH_2O)_3Ge^+$	100	227	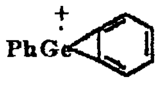	8.3
177	$^n Bu\overset{+}{Sn}$	46	197	$Ph\overset{+}{Sn}$	12.5
147	$PhCH{=}CHCOO^+$	57	177	$^nBu\overset{+}{Sn}$	16.7
121	$H\overset{+}{Sn}$	24.5	147	$PhCH{=}CHCOO^+$	24.1
120	Sn^+	19.9	121	HSn^+	8.3
103	$PhCH{=}\overset{+}{C}H$	44	103	$PhCH{=}\overset{+}{C}H$	13.2

(possibly pentacoordinated geometry) in solution despite differences in solid state.

3.4. Mass spectra

Main fragment ions observed in the mass spectra of compound I_3 and II_2 are listed in Table 6. The molecular ion is never observed but the fragment ions found are in agreement with the expected structure of the compounds. For both compounds, the ions containing germanium (Ph_3Ge^+ or $N(CH_2CH_2O)_3Ge^+$) are the base peaks, and other ions containing germanium are also generally quite intense.

Table 7
Selected bond distances and bond angles of compound I_4^a

Bond	Distances (Å)	Bond	Angles (°)
Sn(1)–O(5)	2.099(6)	O(5)–Sn(1)–O(5a)	81.1(3)
Sn(1)–O(5a)	2.099(6)	O(5)–Sn(1)–O(4)	55.0(3)
Sn(1)–O(4)	2.518(5)	O(5)–Sn(1)–O(4a)	136.0(2)
Sn(1)–O(4a)	2.518(5)	O(5)–Sn(1)–C(8)	27.8(2)
Sn(1)–C(8)	2.659(8)	O(5)–Sn(1)–C(8a)	108.7(3)
Sn(1)–C(8a)	2.659(8)	O(5)Sn(1)–C(21)	106.5(3)
Sn(1)–C(21)	2.10(1)	O(5)–Sn(1)–C(21a)	102.7(3)
Sn(1)–C(21a)	2.10(1)	O(5)–Sn(1)–O(6)	139.5(1)
Sn(1)–O(6)	2.54(4)	O(4)–Sn(1)–O(6)	84.5(2)
Ge(1)–O(1)	1.768(6)	C(21)–Sn(1)–C(21a)	141.2(6)
Ge(1)–O(2)	1.781(5)	C(21)–Sn(1)–O(6)	70.6(3)
Ge(1)–O(3)	1.781(6)	Sn(1)–O(4)–C(8)	82.7(5)
Ge(1)–N(1)	2.222(6)	Sn(1)–O(4)–C(8)	101.5(6)
C(8)–O(4)	1.24(1)		
C(8)–O(5)	1.27(1)		

[a] Numbers in parentheses are estimated standard deviations in the least significant digits.

3.5. Crystal structure of compound II_4

The single crystal was recrystallized from $CHCl_3$/petroether (90–120°C). The crystal structure was deter-

Table 8
Fractional coordinates and thermal parameters of non-hydrogen for compound I_4^a

Atom	x	y	z	B_{eq} (Å^2)
Sn(1)	0.000	0.35506(8)	0.250	3.81(2)
Ge(1)	0.09966(5)	0.17496(8)	−0.08867(5)	3.80(2)
Cl(1)	−0.2221(1)	0.31079(3)	−0.0946(2)	8.6(1)
C(1)	0.1304	−0.017(1)	−0.1759(9)	8.8(4)
C(2)	0.0710(5)	−0.0316(8)	−0.1482(7)	6.0(3)
O(1)	0.0639(3)	0.0439(6)	−0.0873(5)	6.5(2)
C(3)	0.2121(5)	0.117(1)	−0.1596(8)	7.8(3)
C(4)	0.2285(5)	0.138(1)	−0.0755(6)	6.3(3)
O(2)	0.1809(3)	0.1866(7)	−0.0413(4)	6.4(2)
C(5)	0.1137(7)	0.146(2)	−0.2542(7)	11.5(5)
C(6)	0.0908(6)	0.260(1)	−0.2396(6)	6.6(3)
O(3)	0.0714(4)	0.2692(6)	−0.1662(4)	6.5(2)
N(1)	0.1457(4)	0.0991(7)	−0.1831(4)	4.6(2)
C(10)	0.0630(5)	0.2536(8)	−0.0070(6)	4.7(2)
C(11)	−0.0101(5)	0.2649(8)	−0.0275(5)	4.4(2)
C(12)	−0.0511(5)	0.1793(7)	−0.0210(6)	65(2)
C(13)	−0.1162(4)	0.1918(8)	−0.0400(6)	4.8(2)
C(14)	−0.1401(5)	0.2934(9)	−0.0666(6)	4.8(2)
C(15)	−0.1012(5)	0.3795(8)	−0.0718(6)	5.0(2)
C(16)	−0.0354(5)	0.3653(8)	−0.0530(5)	4.7(2)
C(7)	0.0859(5)	0.208(1)	0.0737(6)	5.7(3)
O(5)	0.0367(3)	0.2240(5)	0.1916(3)	4.5(1)
O(4)	0.0640(3)	0.3750(6)	0.1393(4)	5.7(2)
C(8)	0.0611(4)	0.2741(8)	0.1390(6)	4.3(2)
C(21)	0.4243(6)	0.088(1)	0.6642(6)	7.3(3)
C(22)	0.3611(6)	0.066(1)	0.6850(7)	6.4(3)
C(23)	0.6861(5)	−0.013(1)	0.3781(7)	7.1(3)
C(24)	0.2543(6)	0.979(1)	0.6429(8)	8.5(4)

[a] Numbers in parentheses are estimated standard deviations in the least significant digits.

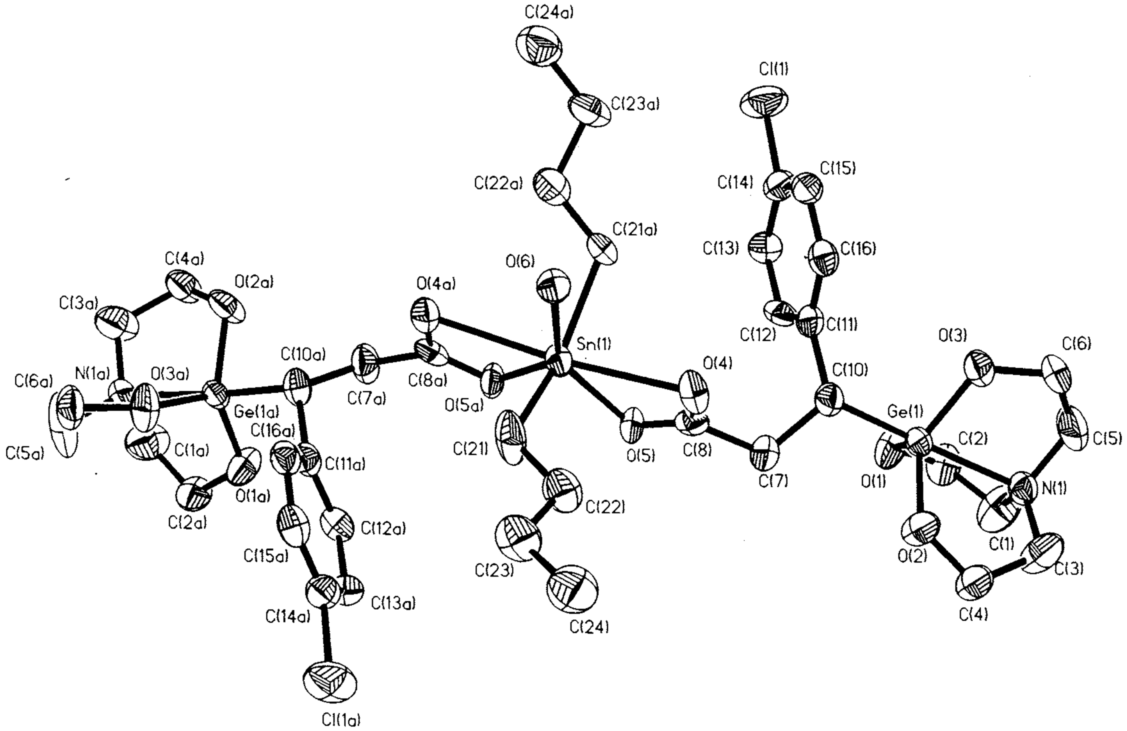

Fig. 1. Molecular structure and crystallographic numbering scheme for $^{n}Bu_2Sn[O_2CCH_2CH(4\text{-}ClC_6H_4)Ge(OCH_2CH_2)_3N]_2.H_2O$.

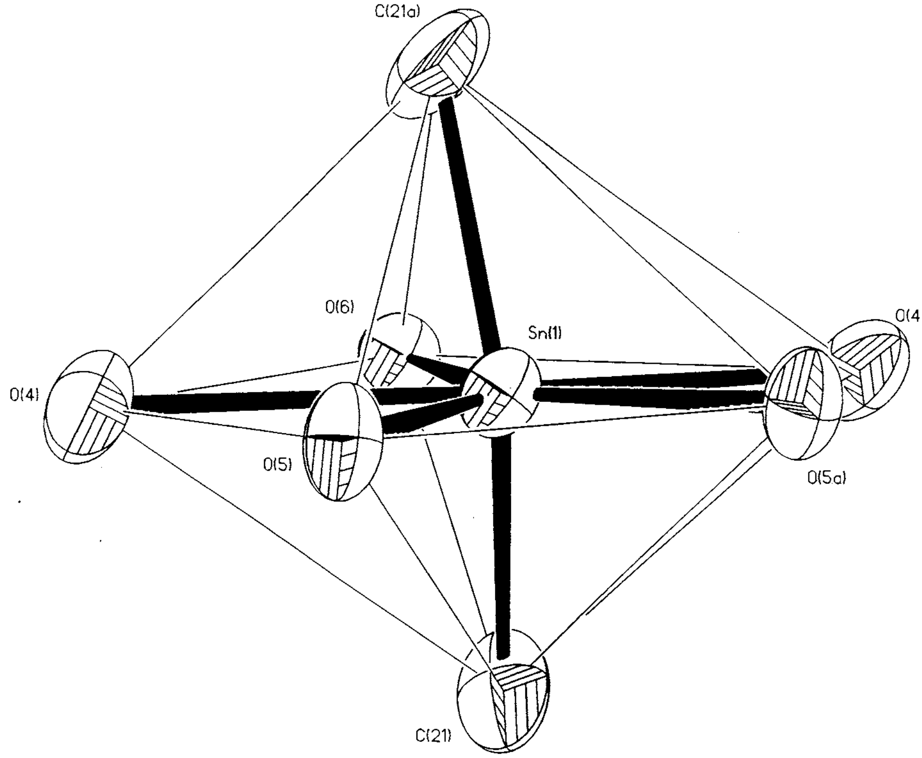

Fig. 2. Pentagonal bipyramidyl structure for C_2SnO_5.

mined by X-ray diffraction. Selected bond lengths and angles are given in Table 7, and the molecular structure with atom numbering of compound II_4 is shown in Fig. 1. We found a water of crystallization in the structure which gives another proof to the possibility of having a water molecule in the product.

The molecule resides on a general position thus giving four formula units per unit cell. The molecular

Table 9
Antitumor activity of selected compounds against KB cells, Bel7402 cells and HCT-8 cells[a]

Compound	10 (μg ml^{-1})			IC_{50} (μg ml^{-1})		
	KB cells	Bel7402 cells	HCT-8 cells	KB cells	Bel7402 cells	HCT-8 cells
I_1	96.2 ± 02	96.2 ± 0.2	93.7 ± 12	5.5	5.5	5.6
I_2	96.9 ± 1.9	92.9 ± 0.5	91.9 ± 0.7	5.4	5.6	4.7
I_4	96.0 ± 0.3	92.7 ± 0.9	91.2	5.5	5.7	5.3
I_5	99.2 ± 1.3	91.9 ± 1.2	95.6 ± 0.3	5.2	5.7	5.7
I_6	95.6 ± 0.3	92.8 ± 0.9	94.9 ± 1.0	5.5	5.6	5.5
I_7	96.9 ± 0.5	96.9 ± 0.5	92.5 ± 0.4	5.4	5.4	4.7
I_8	92.5 ± 0.4	96.1 ± 1.8	92.8 ± 2.5	5.7	5.5	5.7
I_9	94.4 ± 0.9	92.7 ± 0.8	93.1 ± 1.2	—	3.6	5.1
I_{11}	95.7 ± 0.2	93.7 ± 0.3	92.5 ± 1.2	5.5	5.5	5.7
II_1	93.4 ± 0.4	89.8 ± 0.5	89.5 ± 1.8	5.6	5.9	5.9
II_2	89.9 ± 0.3	89.1 ± 0.4	87.6 ± 2.1	5.9	5.9	5.9
II_3	89.1 ± 0.3	87.1 ± 1.7	63.4 ± 4.4	5.9	6.0	6.0
II_4	75.5 ± 2.1	77.7 ± 2.9	89.9 ± 1.7	6.9	6.6	8.1

[a] All compounds have '++', while '+++' stands for good activity.

structure consists of a monomer with a seven-coordinated tin atom surrounded by five oxygens and two butyl groups. The coordination geometry of tin can be described as a pentagonal bipyramid with the plane being defined by four O atoms from two asymmetrically chelating carboxylate groups (Sn(1)–O(5), Sn(1)–O(5a) = 2.099 Å and Sn(1)–O(4), Sn(1)–O(4) = 2.158 Å) and one O atom from the water molecule, while two butyl groups occupying the axial position, with the C–Sn–C angle 141.2°. The pentagon is not regular, three of the five sides, namely that involving O(5)O(5a),O(4)O(6),O(4a)O(6), are remarkably longer than the other two. Consistent with this, the angle subtended at tin by O(5)O(5a),O(4)O(6) and O(4a)O(6) are enlarged to 81.1(3)° 84.5(2)° and 84.5(2)°, respectively, while the other two equatorial angles significantly reduced to 55.0(3)° from that in an idealized pentagonal bipyramid (72°). The largest deviation from the plane of best fit through the five equatorial atoms is 0.0368 Å for O(5) and O(5a), with the tin atom lying exactly on it, while the atom C(21) and C(21a) are away from the plane (± 1.9783 Å). In the crystal structure, two C–O bonds of the carboxylate group have been delocalized, when the two O atoms coordinate to the Sn atom (C(8)–O(4) = 1.24(1) Å, C(8)–O(5) = 1.27(1) Å).

The structure of the title compound is structurally different from those $[R_nSn(O_2CR')_{4-n})$ type complexes in the literature [16], which is described as skew-trapezoidal bipyramid. However, there is a good correspondence in their structural parameters: the short Sn–O distances lie in the range of 2.077–2.156 Å (Sn(1)–O(5), Sn(1)–O(5a) = 2.099 Å), the long Sn–O ones in the range 2.510–2.711 Å (Sn(1)–O(4), Sn(1)–O(4a) = 2.518 Å; Sn(1)–O(6) = 2.54 Å are also in this range). The angles lie in the range 79.5–84.4° for O(5)–Sn(1)–O(5a) (81.1°), 165.3–172° for O(4)–Sn(1)–O(4a) (169.0°), 54.0–55.7 for O(4)–Sn(1)–O(5) and 130.6–147.2° for C(21)–Sn(1)–C(21a) (141.2°).

There is only one example in the literature that reported the crystal structure of *trans*-C_2SnO_5 pentaganol bipyramidal which can be compared with the present one, namely dibutylbis(phenylaceto)tin(IV) hydrate $Bu_2Sn(O_2CCH_2Ph)_2.H_2O$ [17](Fig. 2). Apart from their similarities, the two complexes exhibit some differences that warrant a brief mention. The short Sn–O distance of the carboxylate group is 0.135 Å shorter than that in $Bu_2Sn(O_2CCH_2Ph)_2.H_2O$ (Sn–O, 2.234 Å), while the long Sn–O distance is 0.079 Å longer than that in $Bu_2Sn(O_2CCH_2Ph)_2.H_2O$ (Sn–O, 2.439 Å). The $Sn–O_{water}$ distance of 2.54(1) Å is significantly longer than that in $Bu_2Sn(O_2CCH_2Ph)_2.H_2O$ ($Sn–O_{water}$, 2.432 Å). These differences can be attributed to the mutual repulsions of the two bulky germylpropionate groups in the molecule.

3.6. In vitro tests

A total of 13 of the $^nBu_2Sn(O_2CCHR^1CHR^2GeR_3)_2.H_2O$ compounds were screened in vitro for their antitumor activity against KB cells, HCT-8 cells and Bel7402 cells. The examination of the results summarized in Table 9 suggests the following conclusions:

1. All compounds tested in general show some activity.
2. The Germatrane-substituted derivatives show a higher activity than the $GePh_3$-substituted derivatives.

All compounds are poorly soluble in water. This may be the main reason for their moderate activity.

Acknowledgements

We thank Professor Wang Honggeng and Professor Yao Xinkan for support of the crystallographic study. The National Science Foundation of China is also thanked for support of this research.

References

[1] A.G. Davies, P.J. Smith, in: G. Wilkinson, F.G.A. Stone, E.W. Abel (Eds.), Comprehensive Organometallic Chemistry, vol. 2, Pergamon Press, Oxford, 1982.

[2] C.J. Evans, S. Karpel, Organotin Compounds in Modern Technology, J. Organomet. Chem. Library, vol. 16, Elsevier, Amsterdam, 1985.

[3] S.J. Blunden, P.A. Cussack, R. Hill, The Industrial Use of Tin Chemicals, Royal Society of Chemistry, London, 1985.

[4] I. Omae, Organotin Chemistry, J. Organomet. Chem. Library, vol. 21, Elsevier, Amsterdam, 1989.

[5] V.L. Narayanan, Tin-based Antitumor Drugs, Springer-Verlag, Berlin, 1990, p. 201.

[6] (a) E. Lukevics, Appl. Organomet. Chem. 6 (1992) 113. (b) M.Z. Bai, L.F. Geng, L.J. Sun, Hua Xue Tong Bao 11 (1987) 23.

[7] (a) R. Sato, Jpn. Kokai Tokyo koho 56 (1981) 218. (b) J.V. Scibelli, M.D. Curtis, Synth. React. Inorg. Met.-Org. Chem. 8 (1978) 399.

[8] Y. Kawasaki, T. Tanaka, T.R Okawara, Spect. Acta 105 (1985) 171.

[9] G. Singh, V.D. Gupta, Natl. Acad. Sci. Lett. India 5 (1982) 423.

[10] F. Huber, H. Preut, E. Hoffmann, M. Gielen, Acta Cryst. C45 (1989) 51.

[11] B. Kushlefsky, I. Simmons, A. Ross, Inorg. Chem. 2 (1963) 187.

[12] M. Gielen, M. Melotte, G. Atassi, R. Willem, Tetrahedron 45 (1989) 1219.

[13] R.J. Rao, R. Soneja, L.V. Shastry, S. Sharma, Synth. React. Inorg. Met Org. Chem. 24 (1994) 995.

[14] S.J. Blunden, et al., J. Organomet. Chem 226 (1982) 157.

[15] C. Carini, G. Pellizi, P. Tarasconi, et al., J. Chem. Soc. Dalton Trans. 289 (1989).

[16] E.R.T. Tiekink, Appl. Organomet. Chem. 5 (1994) 1.

[17] S.W. Ng, W. Chen, A. Zainudin, V.G.K Das, W.H. Yip, R.J. Wang, T.C.W. Mak, J. Cryst. Spectr. Res. 21 (1991) 39.